CrossMark

TOPICAL COLLECTION: ELECTRONIC MATERIALS FOR RENEWABLE ENERGY APPLICATIONS

Robust Temperature Control of a Thermoelectric Cooler via μ-Synthesis

BURAK KÜRKÇÜ [1,2,3] and COŞKU KASNAKOĞLU [1,4]

1.—TOBB University of Economics and Technology, Ankara, Turkey. 2.—ASELSAN Inc., Ankara, Turkey. 3.—e-mail: bkurkcu@etu.edu.tr. 4.—e-mail: kasnakoglu@etu.edu.tr

In this work robust temperature control of a thermoelectric cooler (TEC) via μ-synthesis is studied. An uncertain dynamical model for the TEC that is suitable for robust control methods is derived. The model captures variations in operating point due to current, load and temperature changes. A temperature controller is designed utilizing μ-synthesis, a powerful method guaranteeing robust stability and performance. For comparison two well-known control methods, namely proportional-integral-derivative (PID) and internal model control (IMC), are also realized to benchmark the proposed approach. It is observed that the stability and performance on the nominal model are satisfactory for all cases. On the other hand, under perturbations the responses of PID and IMC deteriorate and even become unstable. In contrast, the μ-synthesis controller succeeds in keeping system stability and achieving good performance under all perturbations within the operating range, while at the same time providing good disturbance rejection.

Key words: Robust control, μ-synthesis, thermoelectric cooler, TEC, robust stability, robust performance, disturbance rejection

INTRODUCTION

The thermoelectric effect has received considerable attention lately for its potential of converting heat flux to electrical energy and vice versa.[1] With thermoelectric generators (TEG) it is possible to create electrical potential from temperature difference by the Seebeck effect. As such, it is a form renewable energy since waste heat can be converted back to useful electrical energy. The opposite is possible with thermoelectric coolers (TEC) where an electric potential is used to create a temperature difference by the Peltier effect and thus cool a load.[2] Low-cost materials such as bismuth telluride (Bi_2Te_3) have strong thermoelectric effects which make them useful in the generation of thermoelectric systems.

In terms of popularity, TEC technology today still lacks behind vapor-compression refrigeration. The main benefits of a TEC system over a vapor-compression refrigerator are that there are no moving parts, no liquid circulation is necessary, the life expectancy is long, leaks are not an issue, the size is small and the shape is flexible. Its main drawbacks are high cost and lower efficiency. TEC technology is useful, however, in cases where the solid-state related benefits (e.g. lack of moving parts, cheap maintenance, small size, and the ability to run in any orientation) outweigh efficiency.[3] Examples include portable beverage coolers, water extraction for dehumidification, camping coolers, climate controlled jackets, heat sinks for computers and microprocessors, thermal cyclers, precision laser applications, temperature balancers for spacecraft with one side exposed to direct sunlight, photon detector coolers, wavelength stabilizers for fiber-optics, and various military applications.[4]

Modeling of thermoelectric devices as well as the behavior of materials is an important first step for the design and verification of the device.[5] The model may incorporate electrical, thermodynamic and even mechanical components.[6] One finds numerous works in the literature including the modeling of

thermoelectric material using software such as SPICE,[7,8] dynamical and static modeling of TE modules with MATLAB,[9–11] and customized software to estimate Seebeck and Peltier effects.[12] The effect of thermal properties in the modeling of thermoelectric devices have also been investigated in various studies.[13,14]

The ability to control the cooling characteristics of a TEC is an important task for applications. For certain applications it is adequate to provide basic cooling so precise temperature control is not needed. For these cases simple static models that can provide estimates of a constant voltage/current to be applied are adequate.[10] For other scenarios, it is also possible to obtain successful results with only very basic on/off controllers.[15] For situations where precise temperature regulation is desired, one must utilize more involved dynamical models,[7,16] possibly including electronic elements such as converters driving thermoelectric modules.[17] It is also necessary to implement dynamical controllers such as PID[16] and variants.[18] The main issue with such an approach is the complicated and nonlinear nature of the governing equations of the thermoelectric effect. As a result, one typically linearizes the equations about an operating point to obtain the dynamical models, on which controller design takes place. This makes the design susceptible to variations in the operating point. Moreover there are always parameter uncertainties, neglected dynamics, disturbances and noises. Currently it is difficult to locate systematic methods guiding designers on how to represent such uncertainties, as well as how to build robust controllers for stability and performance under such unfavorable conditions. This makes it difficult for TEC systems to find widespread use in mission-critical tasks.

The aim of this paper is to derive an uncertain dynamical model for a TEC that is amenable to robust control theoretic methods. Of particular interest is μ-synthesis, which is a powerful method in robust control. It guarantees both good stability and performance properties under noise and model uncertainties, both of which are inevitable in real life. In comparison to the studies on the modeling and control of TECs mentioned previously, the main contributions of this paper can be summarized as follows:

1. An uncertain dynamical model is constructed for a TEC. This is differs from obtaining a single (i.e. nominal) transfer function since the uncertain dynamical model captures the effects of all possible uncertainties on the TEC (within limits defined by the designer).
2. A powerful robust control technique, namely μ-synthesis is successfully designed and applied to the TEC using the uncertain dynamical model built. The resulting controller guarantees robust stability and performance. That is, the system will always remain stable and perform well under disturbances and uncertainties within limits set a priori by the designer.

3. The μ-synthesis controller designed is compared with two commonly used (but non-robust) control methods (namely PID and IMC). It is seen that particular uncertainties can potentially destabilize the system under PID and IMC, whereas the μ-synthesis controller remains stable under all possibilities. We believe this is an important point since the literature includes a number of studies on the control of TECs with such non-robust methods, which seem to work well under the particular cases given. It is, however, impossible to test all possible disturbance and uncertainty combinations one by one because there are an infinite number of them. The μ-synthesis framework allows for systematic handling of all possibilities described by the uncertain dynamical model.

The rest of the paper is organized as follows: "Dynamical Model of the ThermoelectricCooler" Section presents the dynamical mathematical model of the thermoelectric cooler. "Controller Theory and Design" Section outlines the how perturbed uncertain model is built and constructs a μsynthesis controller achieving robust stability and performance over uncertainties and disturbances. "Results and Discussion" Section presents simulations to evaluate the results in comparison to two common standard control methods. "Conclusions and Future Works" Section finalizes the paper with conclusions and future research ideas.

DYNAMICAL MODEL OF THE THERMOELECTRIC COOLER

The schematic illustration of a TEC can be seen in Fig. 1.

The TEC comprises of n and p-type semiconductors having low thermal conductivity, metallic interconnections having high electrical/high thermal
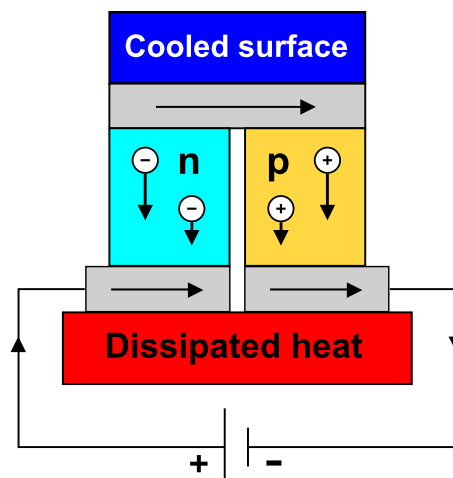

Fig. 1. Schematic illustration of a thermoelectric cooler.

conductivity, and ceramic substrates, which are electrical insulators. Once the external power is provided, current flows through the p-type semiconductor in the direction of the motion of the holes. In the neighboring n-type semiconductor, it flows in the opposite direction of the motion of the electrons. The motion of the holes and electrons transfer energy from the cold region to the hot region, giving the desired cooling effect, known as the Peltier effect.[19]

A dynamical model for the TEC can be obtained from the governing equations as described in Ref. 16, which is briefly summarized here. The temperature distributions within the cold-end plate and within the heat exchanger of the load are approximated as uniform. Applying energy balance to these elements yields

$$(M_L C_L + M_C C_C)\frac{dT_L}{dt} = Q_L - Q_K - I\alpha_{pn}T_L \quad (1)$$

where C_L, M_L are respectively the heat exchanger's heat capacity and mass, C_C, M_C are respectively heat capacity and mass of the cold-end plate, Q_L is the cooling load, I is the current applied to the module, α_{pn} is the Seebeck coefficient of thermoelectric material, and T_L is the thermoelectric module's cold side temperature. Q_K is the cold-end boundary's heat conduction which can be written as

$$Q_K = -kA\frac{\partial T(x,t)}{\partial x}\bigg|_{x=0} \quad (2)$$

where A is the cross-sectional area, $T(x,t)$ is the module's temperature distribution and k is the average thermal conductivity. Applying energy balance to the material results in

$$C\gamma\frac{\partial T(x,t)}{\partial t} = k\frac{\partial^2 T(x,t)}{\partial x^2} - \frac{\tau}{A}I\frac{\partial^2 T(x,t)}{\partial x} + \frac{\rho}{A^2}I^2 \quad (3)$$

where $\tau = Td\alpha_{pn}/dT$ is the Thomson coefficient, ρ is the material's average electrical resistance, C is its average specific heat, and γ is its average density. On the right side of the equation, the second term is related to the heat from Thomson effect. Finally applying energy balance to the hot-side results in

$$(M_F C_F + M_H C_H)\frac{dT_H}{dt} = I\alpha_{pn}T_H + Q_0 \\ - hA_F(T_H - T_a) \quad (4)$$

where M_F, C_F are respectively the mass and heat capacity of the heat sink, M_H, C_H are respectively the hot-end plate's mass and heat capacity, T_H is hot side temperature, h is the heat sink's convective heat transfer coefficient, A_F is its total heat transfer surface area, and T_a is the ambient temperature. Also Q_0 is the hot-side boundary heat conduction which can be written as

$$Q_0 = -kA\frac{\partial T}{\partial x}\bigg|_{x=L} \quad (5)$$

where L is the length of the thermoelectric elements.

The Eqs. 1–5 derived above are thus equations governing the dynamical behavior of a TEC. It is clear that this is a strongly nonlinear model because of temperature dependencies, resistive heat, and Peltier effect. Therefore, it is necessary to linearize the model to obtain small-signal representation so that controller design can be performed on a linear model describing perturbations. For this purpose all the relevant variables of the TEC can be thought of as the sum of a final value and a deviation, i.e.

$$T(x,t) = \bar{T}(x) + \tilde{T}(x,t) \quad (6)$$

$$T_L(T) = \bar{T}_L + \tilde{T}_L(t) \quad (7)$$

$$T_H(T) = \bar{T}_H + \tilde{T}_H(t) \quad (8)$$

$$T_a(T) = \bar{T}_a + \tilde{T}_a(t) \quad (9)$$

$$Q_L(T) = \bar{Q}_L + \tilde{Q}_L(t) \quad (10)$$

$$I(T) = \bar{I} + \tilde{I}(t) \quad (11)$$

where the bar superscript $^-$ denotes the final (steady-state) value and the tilde superscript $^\sim$ denotes the deviation around the steady state. The perturbation $\tilde{T}_L$ is selected as the output to be controlled and the perturbation $\tilde{I}$ is selected as the control input. It is shown in Ref. 16 that linearizing Eqs. 1–5 around the steady-state values and performing some reductions yields a transfer function for the TEC system of the following form

$$\frac{\tilde{T}_L(s)}{\tilde{I}(s)} = -K\frac{s/z + 1}{(s/p_1 + 1)(s/p_2 + 1)} \quad (12)$$

where the parameters K, z, p_1, p_2 can be determined either analytically or experimentally. For the purposes of this study it is more convenient to utilize a set of experimentally determined coefficients at different operating conditions as given in Table I.

It is observed from the table that the parameters vary considerably with changes in the operating point. The operating point will inevitably change during the operation of the TEC as the currents, cooling load and temperatures vary. One possible approach that is commonly utilized in TEC literature is to compute a *nominal system* by averaging over all the parameters. For the values K, z, p_1, p_2 in the table this yields the nominal plant

$$P(s) = -\bar{K}\frac{s/\bar{z} + 1}{(s/\bar{p}_1 + 1)(s/\bar{p}_2 + 1)} \quad (13)$$

where the averaged parameters are $\bar{K} = 6.4061$, $\bar{z} = 0.1323$, $\bar{p}_1 = 0.0147$, $\bar{p}_2 = 0.5817$. A controller design (typically PID) is then be carried out on this

Table I. Parameters K, z, p_1, p_2 at multiple operating points $\bar{I}$(A), $\tilde{I}$(A), Q_L (W), $\bar{T}_L$ (°C) (Data from Ref. 16)

$\bar{I}$	$\tilde{I}$	Q_L	$\bar{T}_L$	K	z	p_1	p_2
1.5	0.5	0	− 6.0	9.5566	0.1375	0.0115	0.5379
1.5	0.5	5	2.5	10.1439	0.1360	0.0104	0.5226
1.5	0.5	10	11.7	11.0872	0.1421	0.0108	0.5907
2.25	0.5	0	− 10.1	5.6163	0.1317	0.0135	0.4847
2.25	0.5	5	− 1.5	6.0544	0.1293	0.0134	0.5018
2.25	0.5	10	7.2	7.0804	0.1314	0.0125	0.5500
3.0	1.0	0	− 14.4	2.3927	0.1319	0.0213	0.6600
3.0	1.0	5	− 6.8	2.6693	0.1247	0.0197	0.6407
3.0	1.0	10	1.6	3.0541	0.1262	0.0193	0.7486

model to regulate the cold side temperature using the current. Since the controller design is carried out for a point in the center of the operating region, the designer hopes that the controller will remain valid for the entire operating range. This may indeed be the case for many applications, but there is always the risk that a peculiar combination of $\bar{I}$, Q_L and $\bar{T}_L$ will create problems, even cause instability. In the succeeding section we show that this possibility is quite real for the TEC described by the data in Table I. A PID controller working satisfactorily for the nominal (averaged) parameters is shown to produce instability for certain parameter combinations within the operating range. An alternative controller design, namely internal model control (IMC) is also implemented where it is seen that a similar instability occurs. This motivates and justifies the need to consider robust designs, i.e. the need to explicitly model uncertainties and take them into account when controlling the TEC. Thus a controller design utilizing a powerful robust control method, namely μ-synthesis is implemented. It is seen that the μ-synthesis-controlled TEC system remains stable and retains good performance under all possible uncertainties within the operating range.

CONTROLLER THEORY AND DESIGN

As described in the preceding section, although the transfer function model in (13) may be sufficient in the nominal case, in many practical systems, the dynamics of the plant can vary considerably through various operating conditions.[20] In such cases it is unacceptable to represent the behavior of the system only with the nominal model due to this variation. Moreover, uncertainties due to parameter errors, approximations made during modeling, disturbances and noises should also be accounted for. To represent the entire dynamics while incorporating all of these effects, we first define a plant family that includes all possible plants, i.e a perturbed plant family $\hat{P}$, as follows

$$\hat{P} \in \left\{ P(1 + \Delta W_T) \quad | \quad \forall\, \|\Delta\|_\infty \le 1 \right\} \qquad (14)$$

where W_T is a robustness weight function and Δ is any stable, infinity norm-bounded, unstructured uncertainty function. The function W_T must be stable and strictly proper. A generic way to describe the robustness weight function W_T, which will be used in this paper is given in Ref. 21 as follows

$$\left| \frac{M_{ik} e^{j\phi_{ik}}}{M_i e^{j\phi_i}} - 1 \right| \le |W_T(j\omega_i)| \qquad (15)$$
$$\text{for } i = 1, \ldots, m; \quad k = 1, \ldots, n$$

where the phase and magnitude are obtained at ω_i (for $i = 1, \ldots, m$) and the experiment is redone n times based on the application (in this case, the number these experiments is related with the number of operating points). (M_{ik}, ϕ_{ik}) denotes the magnitude–phase pair measurements for frequency ω_i and experiment k. (M_i, ϕ_i) denotes the magnitude–phase pairs for the nominal plant P. In the next subsection, the aim is design a controller that can satisfy both stability and performance criteria for all possible perturbations as described by (14).

μ-Synthesis

Numerous applications of robust control for handling uncertainties exist including autopilots for aircrafts,[22,23] voltage regulators for photovoltaic systems[24] and control of proton-exchange membrane fuel cells.[25] Here we implement the robust control through μ-synthesis, one of the strongest methods for achieving robust stability and performance.[26,27] The proposed control structure as a block diagram is given in Fig. 2.

The definition of the sensitivity (S) and complementary sensitivity (T) functions for the nominal system are given as

$$S(s) = \frac{1}{1 + PK_\mu}, \quad T(s) = \frac{PK_\mu}{1 + PK_\mu} \qquad (16)$$

The aim is to design a controller K_μ for the system $\hat{P}$ to satisfy the robust performance objective with respect to performance weight W_P and robustness weight W_T. A possible way to define W_P is given in Ref 26 as

Fig. 2. Block diagram representation of the proposed control structure.

$$W_P(s) = \left(\frac{s/\sqrt[k]{M_p} + \omega_b}{s + \omega_b \sqrt[k]{\xi_p}} \right)^k \quad (17)$$

where ω_b is the cut-off frequency for the sensitivity function, M_p is maximum permissible overshoot for W_P, $\xi_p \ll 1$ ensures approximate integral action for the sensitivity function and k is an integer greater than 1. In addition, the system M is a standard second order reference dynamics for the system and the performance of the system is minimized based on how close it is to the desired dynamic response. The structure of the M is given as

$$M(s) = \frac{\omega_n^2}{s^2 + 2\xi\omega_n s + \omega_n^2} \quad (18)$$

where ω_n denotes the natural frequency and ξ is the damping ratio of the reference response. W_U is the allowed frequency based control effort weight. This function provides limits to the control usage dictated by physical restrictions of the problem. A general form for the weight W_U is

$$W_U(s) = \left(\frac{s + \omega_u/\sqrt[k]{M_u}}{s\sqrt[k]{\xi_u} + \omega_u} \right)^k \quad (19)$$

where ω_u is the cut-off frequency for $K_\mu S_\mu$, M_u is the maximum permissible input usage for $K_\mu S_\mu$, $\xi_u \ll 1$ prevents high frequency control input usage and k is some integer greater than 1.

The control system configuration for μ-synthesis is shown in Fig. 3 where w_μ is the reference input (r), u_μ is the control input, d_μ is the output of the unstructured uncertainty, v_μ is the input of the unstructured uncertainty, e_μ is the error fed to the controller and z_μ is the output of the interconnection

Fig. 3. Control system configuration for μ-synthesis.

matrix formed as $[e_y \ e_u]^T$. To obtain the open-loop interconnected transfer function matrix (G_μ), the following derivations based on Fig. 2 are given as

$$v_\mu = W_T u_\mu$$
$$e_y = W_P P u_\mu + W_P P d_\mu - W_P M w_\mu, \quad e_u = W_U u_\mu$$
$$\Rightarrow z_\mu = \begin{bmatrix} e_y \\ e_u \end{bmatrix} = \begin{bmatrix} -W_P M \\ 0 \end{bmatrix} w_\mu + \begin{bmatrix} W_P P \\ W_U \end{bmatrix} u_\mu + \begin{bmatrix} W_P P \\ 0 \end{bmatrix} d_\mu$$
$$e_\mu = w_m u_\mu - P d_\mu - P u_\mu$$

$$(20)$$

Note that the interconnection matrix is formed as

$$\begin{bmatrix} v_\mu \\ e_y \\ e_u \\ e_\mu \end{bmatrix} = G_\mu \begin{bmatrix} d_\mu \\ w \\ u_\mu \end{bmatrix} \Rightarrow \begin{bmatrix} v_\mu \\ e_y \\ e_u \\ e_\mu \end{bmatrix} = \begin{bmatrix} G_{\mu,11} & G_{\mu,12} \\ G_{\mu,21} & G_{\mu,22} \end{bmatrix} \begin{bmatrix} d_\mu \\ w \\ u_\mu \end{bmatrix}$$

(21)

The extended version of G_μ is

$$\mathbf{G}_\mu = \begin{bmatrix} 0 & 0 & W_T \\ W_P P & W_P M & W_P P \\ 0 & 0 & W_U \\ -P & -I & -P \end{bmatrix}.$$

(22)

The blocks $G_\mu(s)$ and $K_\mu(s)$ can be combined into block N_μ as:

$$\begin{aligned} \mathbf{N}_\mu &= \mathcal{F}_l(\mathbf{G}_\mu, K_\mu) \\ &= \mathbf{G}_{\mu,11} + \mathbf{G}_{\mu,12} K_\mu (\mathbf{I} - \mathbf{G}_{\mu,22} K_\mu)^{-1} \mathbf{G}_{\mu,21} \\ &= \begin{bmatrix} -W_T T & -W_T K_\mu S \\ W_P P S & W_P(M-T) \\ W_U T & W_U K_\mu \end{bmatrix}. \end{aligned}$$

(23)

The purpose is to obtain a stabilizing controller K_μ satisfying the following expression[28]

$$\sup_\omega \mu[N_\mu(j\omega)] < 1$$

(24)

where μ denotes structured singular values.[26] This can be expressed as the optimization problem

$$\inf_{K_\mu(s)} \sup_\omega \mu[N_\mu(j\omega)] < 1 .$$

(25)

where inf denotes the infimum and sup denotes the supremum of a given function. A common numerical approach to attack (25) is the D–K iteration method which is based on solving

$$\inf_{K_\mu(s)} \sup_\omega \inf_D \bar{\sigma}[DN_\mu D^{-1}(j\omega)].$$

(26)

To achieve (24), a stabilizing controller is to be found such that

$$\sup_\omega \inf_D \bar{\sigma}[DN_\mu D^{-1}(j\omega)] < 1.$$

(27)

For a fixed D, an H_∞ optimization problem can be formed as

$$\inf_{K_\mu(s)} \|DN_\mu D^{-1}\|_\infty \Leftrightarrow \inf_{K_\mu(s)} \|DF_l(G_\mu, K_\mu)D^{-1}\|_\infty$$
$$= \inf_{K_\mu(s)} \|F_l(G_\mu^{scaled}, K_\mu)\|_\infty$$

(28)

where

$$G_\mu^{scaled} = \begin{bmatrix} D & 0 \\ 0 & -I \end{bmatrix} G_\mu \begin{bmatrix} D^{-1} & 0 \\ 0 & -I \end{bmatrix}.$$

(29)

The procedure for D–K iteration can be summarized in the following steps
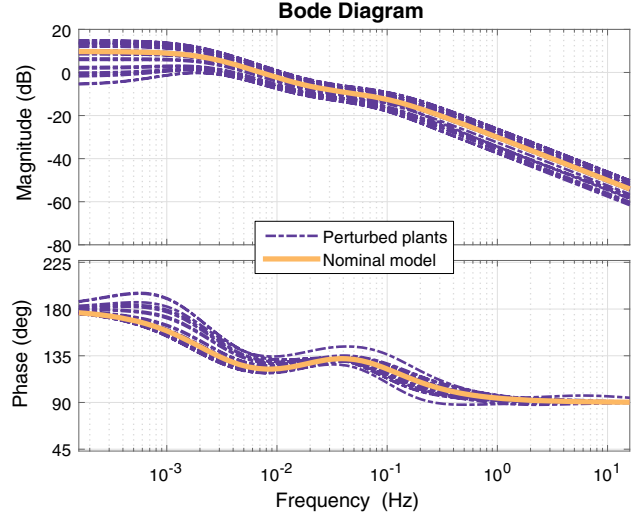

Fig. 4. Bode diagram of the nominal and perturbed plant models for the TEC.

1. Begin with an first estimate for D, e.g. $D = I$.
2. Let D be constant and obtain the solution to the H_∞ problem for K_μ

$$K_\mu = \arg\inf_{K_\mu} \|F_l(G_\mu^{scaled}, K_\mu)\|_\infty .$$

(30)

3. Taking K_μ as constant, solve at each ω of a frequency range of interest the following problem

$$D(j\omega) = \arg\inf_D \bar{\sigma}[DF_l(G_\mu, K_\mu)D^{-1}(j\omega)] .$$

(31)

4. By curve fitting $D(j\omega)$, obtain a stable and minimum phase $D(s)$. Then, repeat the procedure from Step 2 and repeat the procedure, until an acceptable convergence tolerance is met.

RESULTS AND DISCUSSION

μ-Synthesis Implementation

The first step is to build the uncertain model for the system as given in (14). This is achieved by first writing out the transfer functions of all the operating conditions given in Table I, observing their frequency responses and then selecting an uncertainty weight W_T so that the error on the nominal model (13) for all cases is covered by this uncertainty weight. The Bode diagrams of all perturbed plants denoted as $\hat{P}$ are shown by Fig. 4 together with the nominal model.

The robustness weight W_T is then derived by following the idea in (15). The analytic expression of the weight function $W_T(s)$ fitted is
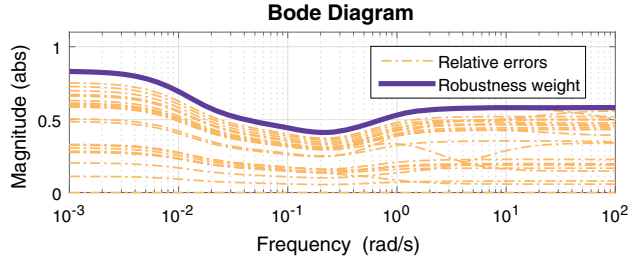
Bode Diagram

Fig. 5. The robustness weight W_T and relative errors of identified models.

Bode Diagram

Fig. 6. The sensitivity, complementary sensitivity and control effort functions.

Bode Diagram
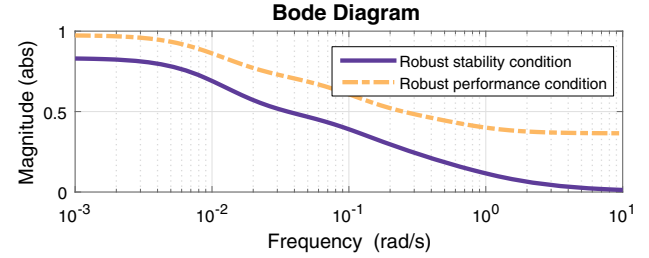
Fig. 7. μ values of the closed-loop system for robust performance and robust stability.

$$W_T(s) = \frac{0.58s^4 + 0.32s^3 + 0.04s^2 + 0.001s + 0.00002}{s^4 + 0.76s^3 + 0.10s^2 + 0.003s + 0.00002}$$

This weight function and relative errors between the nominal model and operating points are plotted in Fig. 5 where it can be seen that all the uncertainty is covered.

The reference model is chosen as a second order system $M(s)$ with $\omega_n = 0.5$ and $\xi = 1$ as follows

$$M(s) = \frac{0.25}{s^2 + s + 0.25}. \tag{32}$$

The performance weight W_P and control input weight W_U are chosen as follows

$$W_P(s) = \frac{s + 0.2}{2s + 0.0002} \tag{33}$$

and

$$W_U(s) = \left(\frac{(s+10)/\sqrt[3]{5}}{s\sqrt[3]{0.0001} + 10} \right)^2. \tag{34}$$

At this point the system is amenable to the D–K iteration outlined in "μ-Synthesis Section. The procedure was implemented numerically utilizing MATLAB to construct the controller K_μ as follows

$$K_\mu(s) = \frac{-40.456(s + 0.01471)(s + 0.5819)(s^2 + 0.9067s + 0.2259)}{s(s + 35.07)(s + 0.1574)(s^2 + 0.9241s + 0.2187)}$$

satisfying $\sup_\omega \mu[N_\mu(j\omega)] < 0.9372$, which is less than one, indicating a successful design. The closed-loop system characteristics and the controller can now be demonstrated in terms of singular values. The sensitivity S, complementary sensitivity T and control effort KS of the resultant system are given in Fig. 6.

Based on these functions μ-analysis is employed, which gives information about closed-loop robust stability (RS) and robust performance (RP). The results are given in Fig. 7.

It can be confirmed that under this controller the uncertain system is robustly stable against the modeled uncertainty. It can in fact remain stable up to 120% of the modeled uncertainly.
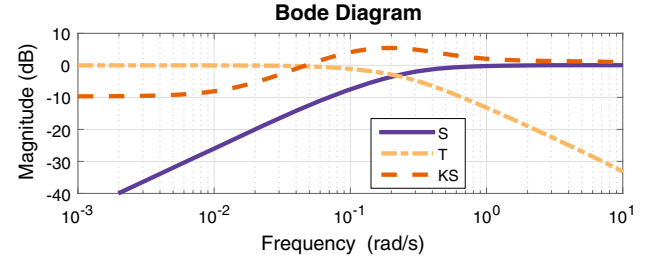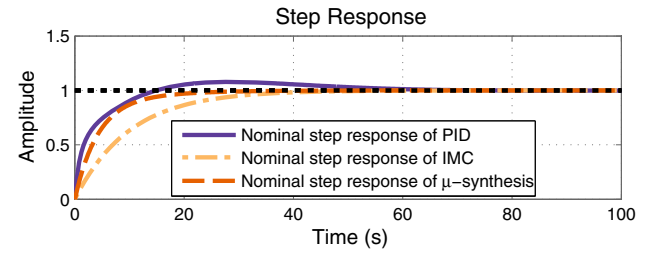
Step Response

Fig. 8. Responses of the nominal system to a reference step input.

Comparison to PID and IMC

In this section, two well-known standard control design techniques, proportional-integral-derivative (PID) and internal model control (IMC)[29] are employed to benchmark the power of the proposed approach. The design of the PID control was done via the well-known and widely used Ziegler–Nichols automated tuning method resulting in

$$K_{PID} = K_P + \frac{K_I}{s} + K_D s \tag{35}$$

where $K_P = -2.96$, $K_I = 11$ and $K_D = 0$. The IMC control was implemented in MATLAB using the procedure in Ref. 29 with time constant $\tau = 10$ resulting in

$$K_{IMC} = \frac{-0.50609(s + 0.01471)(s + 0.5819)}{s(s + 0.1323)} . \tag{36}$$

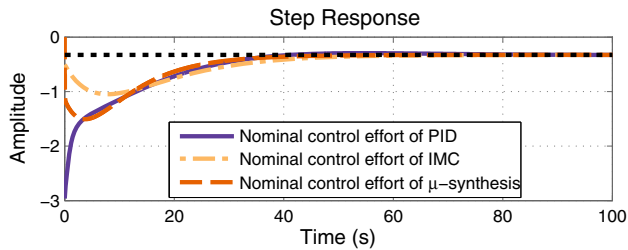A comparison is performed for two cases: first the nominal plant and then the perturbed plant. The

Step Response

Fig. 9. The control effort of three controllers for a given step reference input.
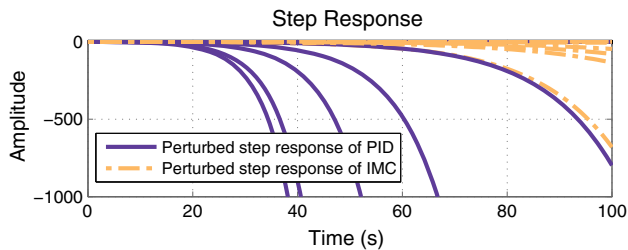
Step Response

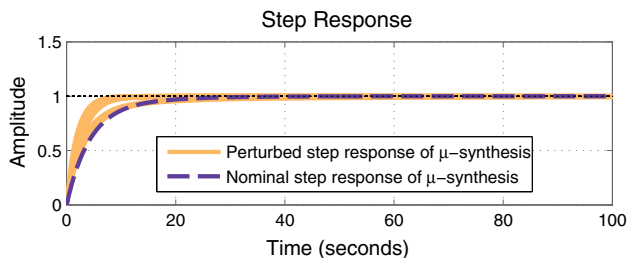Fig. 10. Reference step input to perturbed system and the responses for PID and IMC.

Step Response

Fig. 11. Reference step input to perturbed system and the response for μ-synthesis.
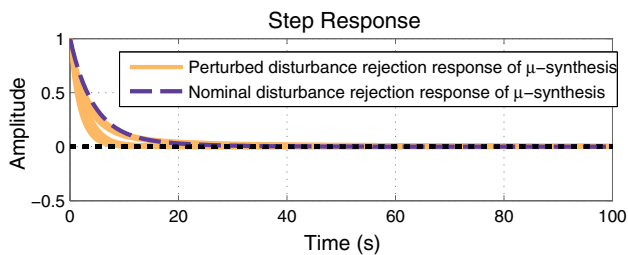
Step Response

Fig. 12. Disturbance rejection behavior of the perturbed system for μ-synthesis.

result of the nominal case for a given step reference input is shown in Fig. 8 together with the control efforts in Fig. 9.

The response of μ-synthesis has no overshoot and it seems faster compared with PID and IMC. Still, all of these responses could be acceptable based on the application at hand. The difference lies in the

perturbed system responses shown for PID and IMC in Fig. 10. Certain perturbations are seen to destabilize the TEC system under these controllers, which is undesired and could lead to fatal outcomes.

In contrast the step response of the perturbed system controlled by μ-synthesis is given in Fig. 11.

It is clear that the stability is retained for all possible operating conditions captured by the perturbed model. In addition good performance is achieved for all perturbations, with no overshoot and settling time less that 20 s. Finally the closed-loop disturbance rejection behavior is investigated. The analysis is meaningful only for μ-synthesis since the other two controllers do not satisfy robust stability. The step disturbance rejection behavior is shown in Fig. 12 where it is seen that a disturbance applied to the system is rejected within 20 s for all possible operating conditions.

The results seem to support that the outlined modeling and control approach, in comparison to alternate standard non-robust options, provides improvements in the direction of high closed-loop stability, performance and disturbance rejection under the presence uncertainties and operating condition variations.

CONCLUSIONS AND FUTURE WORKS

In this work an uncertain dynamical model was built for a thermoelectric cooler (TEC) and its robust control through μ-synthesis was investigated. A robustness weight is determined to cover numerous transfer functions at multiple operating points resulting in a perturbed family of plants. μ-synthesis design was carried out and was seen to be successful under all operating conditions at retaining stability, delivering good performance and rejecting disturbances. Two simpler and common control design techniques, namely PID and IMC were also implemented as benchmarks. It was seen that while PID and IMC also perform satisfactorily under average nominal conditions, certain perturbations within allowed limits cause problems and even instability. As such, the outlined approach provides contributions that could benefit scientists interested in the modeling and robust control of TEC systems.

Future research directions include investigating other controller design methods to TEC systems, as well as improving the uncertain perturbed models.

REFERENCES

1. F.J. DiSalvo, *Science* 285, 5428, 703 (1999).
2. R.A. Taylor and G.L. Solbrekken, *IEEE Trans. Compon. Packag. Technol.* 31, 1, 23 (2008).
3. P. Bansal and A. Martin, I*nt. J. Energy Res.* 24, 2, 93 (2000).
4. S.B. Riffat and X. Ma, *Appl. Therm. Eng.* 23, 8, 913 (2003).
5. R. McCarty, *J. Electron. Mater.* 39, 9, 1842 (2010).
6. F. Felgner, L. Exel, M. Nesarajah, and G. Frey, *IEEE Trans. Ind. Electron.* 61, 3, 1301 (2014).
7. S. Lineykin and S. Ben-Yaakov, *IEEE Power Electron. Lett.* 3, 2, 63 (2005).

8. C. Li, D. Jiao, J. Jia, F. Guo, and J. Wang, *IEEE Trans. Ind. Appl.* 50, 6, 3995 (2014).

9. A. Yusop, R. Mohamed, A. Ayob, and A. Mohamed, *Model. Simul. Eng.* 2014, 22 (2014).

10. H.L. Tsai and J.M. Lin, *J. Electron. Mater.* 39, 9, 2105 (2010).

11. K. Kobbekaduwa and N. Subasinghe, *Int. J. Energy Power Eng.* 5, 3, 97 (2016).

12. C.N. Kim and J. Kim, *J. Electron. Mater.* 44, 10, 3586 (2015).

13. J. Chavez, J. Ortega, J. Salazar, A. Turo, and M.J. Garcia, in *Proceedings of the 17th IEEE Instrumentation and Measurement Technology Conference*, 2000. IMTC 2000. vol. 2 (IEEE, 2000), pp. 1019–1023.

14. K.H. Lee, H. Kim, and O.J. Kim, *J. Electron. Mater.* 39, 9, 1566 (2010).

15. D. Astrain, A. Martínez, J. Gorraiz, A. Rodríguez, and G. Pérez, *J. Electron. Mater.* 41, 6, 1081 (2012).

16. B. Huang and C. Duang, *Int. J. Refrig.* 23, 3, 197 (2000).

17. K. Sun, H. Wu, Y. Cai, and Y. Xing, *J. Electron. Mater.* 43, 6, 2287 (2014).

18. S.J. Song and J.J. Wang, *Applied Mechanics and Materials* (Stafa-Zurich: Trans Tech Publ, 2012), vol. 130, pp. 1919–1924.

19. M.J. Moran, H.N. Shapiro, D.D. Boettner, and M.B. Bailey, *Fundamentals of engineering thermodynamics* (New York: Wiley, 2010).

20. B. Kürkçü and C. Kasnakoğlu, *Applied Mechanics and Materials* (Stafa-Zurich: Trans Tech Publ, 2015), vol. 789, pp. 951–956.

21. J.C. Doyle, B.A. Francis, and A.R. Tannenbaum, *Feedback control theory* (North Chelmsford: Courier Corporation, 2013).

22. S. Akyurek, G.S. Ozden, B. Kurkcu, U. Kaynak, C. Kasnakoglu, in *2015 9th International Conference on Electrical and Electronics Engineering (ELECO)* (IEEE, 2015), pp. 790–795.

23. Ş. Akyürek, B. Kürkçü, Ü. Kaynak, and C. Kasnakoğlu, *IFAC-PapersOnLine* 49, 9, 117 (2016).

24. O. Deveci and C. Kasnakolu, *Int. J. Hydrog. Energy* 42, 28, 18064 (2017).

25. F.C. Wang and C.C. Ko, *Int. J. Hydrog. Energy* 35, 19, 10437 (2010).

26. K. Zhou and J.C. Doyle, *Essentials of Robust Control* (Upper Saddle River: Prentice hall, 1998), vol. 104.

27. Z. Chen, B. Yao, and Q. Wang, *IEEE/ASME Trans. Mechatron.* 20, 3, 1482 (2015).

28. S. Skogestad and I. Postlethwaite, *Multivariable Feedback Control: Analysis and Design* (New York: Wiley, 2007).

29. M. Morari and E. Zafiriou, *Robust Process Control* (Englewood Cliffs: Prentice hall, 1989).